

Comparison of visual and acoustic surveys for the detection and dynamic management of North Atlantic right whales (*Eubalaena glacialis*) in Canada

Valentina Ceballos  | Christopher Taggart | Hansen Johnson 

Oceanography Department, Dalhousie University, Halifax, Nova Scotia, Canada

Correspondence

Valentina Ceballos, Oceanography Department, Dalhousie University, 1355 Oxford Street, Halifax, Nova Scotia, B3H 4R2, Canada.
Email: valentina.ceballos@dal.ca

Funding information

Dalhousie University, Grant/Award Numbers: Killam Predoctoral Scholarship, Nancy Witherspoon Memorial Summer Research Award, Nova Scotia Graduate Research Scholarship, President's Award, Rob Stewart Award in Marine Conservation; Natural Sciences and Engineering Research Council of Canada, Grant/Award Number: Vanier Canada Graduate Fellowship

Abstract

The goal of this study was to develop a simulation to quantitatively compare acoustic and visual surveys and use it to inform current and future North Atlantic right whale (*Eubalaena glacialis*) risk mitigation. We expanded upon an established whale movement model, incorporating realistic right whale cues for visual and acoustic detection within dynamic management zones in the Gulf of Saint Lawrence, Canada. Survey transits by acoustic (Slocum gliders) and visual (aircraft, vessels, and Remotely Piloted Aircraft Systems) platforms were simulated using representative platform movements and detection functions. We used a Monte Carlo approach to estimate the probability of detecting a cue, in each zone, as a function of survey platform, number of right whales, and survey transits. Acoustic gliders detected right whale presence in every scenario. Single transits of a management zone by visual surveys were only able to reliably (>0.5 probability) detect right whales when more than 20 whales were present. Twenty or more transits were required to reliably detect a single right whale. Our results serve as a tool to be used by decision-makers to inform optimal right whale monitoring strategies that consider the relative strengths of the various platforms.

KEYWORDS

dynamic management, passive acoustic monitoring, right whale, visual survey

1 | INTRODUCTION

The North Atlantic right whale (*Eubalaena glacialis*; hereafter “right whale”) was subjected to intense commercial hunting pressure for 100 of years. Despite placing a moratorium on commercial whaling in 1935 (DFO, 2008) and the subsequent listing of the species as endangered under the Canadian Species at Risk Act (SARA) in 2005 (DFO, 2021a), right whales have not

recovered. In fact, their numbers have experienced a significant decline since approximately 2010 (Pettis et al., 2022). In 2020, it was presumed that 336 individuals of the species were alive, with less than 90 breeding females in 2021 (Pettis et al., 2022). This strongly contrasts with their pre-whaling numbers of between 9000 and 20,000 (Monsarrat et al., 2016).

The contemporary threats that right whales face are numerous, the most severe of which primarily arise from

This is an open access article under the terms of the [Creative Commons Attribution](https://creativecommons.org/licenses/by/4.0/) License, which permits use, distribution and reproduction in any medium, provided the original work is properly cited.

© 2022 The Authors. *Conservation Science and Practice* published by Wiley Periodicals LLC on behalf of Society for Conservation Biology.

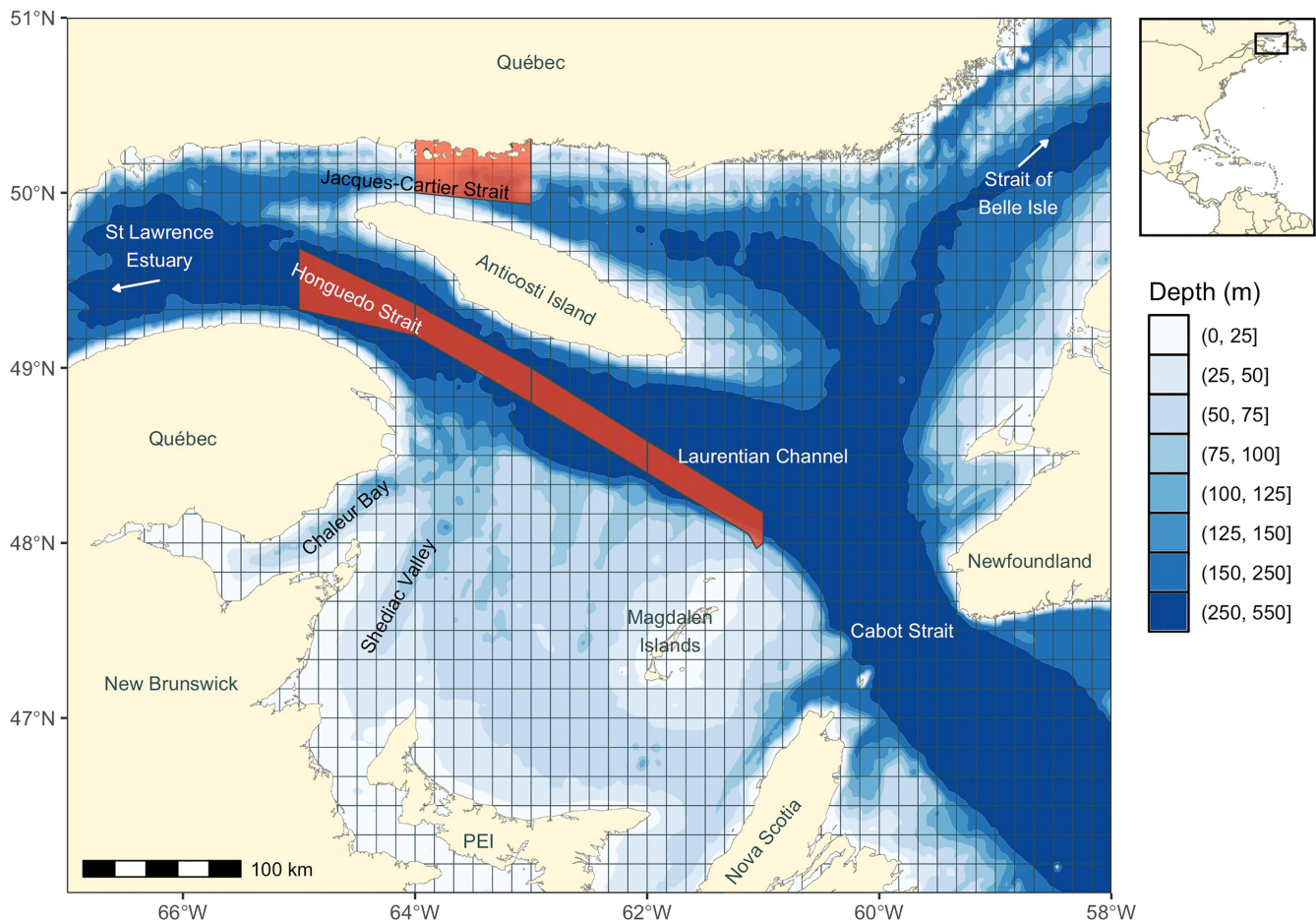


FIGURE 1 Bathymetric chart of the Gulf of Saint Lawrence (GSL) illustrating DFO and TC dynamic management zones from the 2020 management plan. The DFO fisheries zones are laid out in a grid and span the GSL, from the U.S. to the Cabot strait; a singular zone (small gray rectangular outline) was used to model our 18 by 12-km DFO simulation domain. There exist five TC transit speed restriction zones around Anticosti Island (red); a singular zone was used to model our 100 by 20-km TC simulation domain. Bathymetry acquired from the “ETOPO1” dataset (NOAA, 2009); scale is in km

anthropogenic activities, namely fishing gear entanglements and vessel strikes (Pettis et al., 2022). For example, all detected right whale mortalities between 2003 and 2018 in Canadian and U.S. waters for which the cause of death could be determined were caused by one of these two factors (Sharp et al., 2019). In addition, a combination of supplementary stressors, such as sub-lethal entanglement and poor food resources, negatively impact individual health and reproduction (Moore et al., 2021). A shift in right whale distribution beginning around 2010 exacerbated these impacts by bringing the species into contact with unmitigated risks in new areas, specifically the Gulf of Saint Lawrence (GSL; Davies & Brillant, 2019). This shift was likely driven by climate-induced changes in the availability of *Calanus finmarchicus* copepods (Record et al., 2019), an important food source for right whales (e.g., Baumgartner et al., 2003). These issues are linked to the unprecedented mortality event that began in 2017 (NOAA, 2021), where

17 individuals, ~4% of the total population, were found dead, 12 of them in Canadian waters, and the additional 10 individuals that were found dead in 2019, nine of them in Canada (Pettis et al., 2022).

These mortality events prompted the implementation of strict, extensive management measures in Canada as an effort to reduce risk to this species (Davies & Brillant, 2019). Many of these measures are dynamic in nature, meaning they affect and restrict activities in sectors, mostly of the GSL, throughout a season and can change multiple times over a matter of days or weeks. Fisheries and Oceans Canada (DFO) and Transport Canada (TC) each established dynamic management zones in the GSL affecting where and how fishers and vessels are permitted to operate. DFO applies dynamic fisheries management measures to fixed gear fisheries (e.g., snow crab, lobster; DFO, 2021b) in the ~12 × 18 km grid cell zones located from the U.S. boundary to north of Newfoundland (DFO, 2020;

Figure 1). TC applies dynamic vessel management measures among five larger zones ($\sim 20 \times 100$ km) located in the shipping corridors north and south of Anticosti Island (TC, 2020; Figure 1). Although the DFO and TC zones are relatively consistent over time, various changes to these risk-mitigation measures may be implemented in particular zones within and among years. All such measures explicitly rely upon near real-time detections of right whales.

Near real-time detections of right whales are typically made using either visual or passive acoustic monitoring (PAM) surveys. Visual surveys, conducted by aircraft, vessels, or remotely piloted aircraft systems (RPAS), can provide essential conservation information, such as whale abundance, identity, health, mortality, population genetics, and behavior (Pettis et al., 2022). Such surveys are costly and subject to many challenges such as limited endurance, whale visibility, inclement weather, and risk to human operators. Right whale presence can also be accurately determined using near-real time PAM, where platforms equipped with an omnidirectional hydrophone and a classification system can monitor for right whale calls and transmit the detection information in near real-time. PAM platforms used to indicate right whale presence include static ones, such as moored buoys, as well as mobile ones, such as autonomous ocean profilers like Slocum gliders (e.g., Baumgartner et al., 2020). Slocum gliders are fitted with an array of sensors to monitor given locations and depths regionally, moving in a sawtooth pattern in the water column via buoyancy control, and surfacing to transmit their data (Schofield et al., 2007). Acoustic surveys like these typically monitor persistently over long periods (weeks to months) at comparatively low costs and with limited platform deployment and recovery risks to human operators. However, PAM systems on Slocum gliders cannot currently provide precise locations of right whale individuals or reliable estimates of animal density, nor can they collect additional conservation data typically available to visual surveys (e.g., photographic identification, demographics, health condition).

The Government of Canada uses either a single visual or acoustic whale detection from these various survey platforms to trigger dynamic management measures, but while efforts to coordinate and optimize regional right whale management are ongoing, visual surveys are still the most common right whale monitoring strategy (Johnson et al., 2021). So, to truly attempt to better right whale conservation, it is important to evaluate and compare each methodology, and whale availability and detection biases must be considered. Availability biases are factors that affect the probability that a given cue (e.g., whale call or surfacing) is available for detection,

whereas detection biases are factors that affect the probability of detecting an available cue. The primary source of availability bias for visual surveys is the requirement that whales be at or near the surface (Thomson et al., 2013); for acoustic surveys, that a whale produces a call (Marques et al., 2013). Detection biases in right whale monitoring in large part arise from unequal monitoring efforts, with acoustic surveys spending more time in the water compared to their visual counterparts. Other sources of detection biases also include effects such as day versus night, poor visibility and sea state during visual surveys (e.g., Clark et al., 2010) or sources of noise during acoustic surveys, including other species calls, that can mask right whale calls and interfere with the ability to detect a given call (e.g., Johnson et al., 2022).

The above biases make it difficult to directly compare visual and acoustic survey results in the field. Thus, we employ a simulation-based approach using an agent-based model to overcome the difficulty. Agent-based models assign a specific set of rules to autonomous agents to represent complex systems and have been widely and successfully applied for conservation applications (McLane et al., 2011), including in right whale conservation (Johnson et al., 2020; van der Hoop et al., 2012). We expand upon the agent-based models developed and used by van der Hoop et al. (2012) and Johnson et al. (2020) to account for availability and detection biases in acoustic and visual surveys, focusing on the mobile platforms currently being used and developed for right whale monitoring in the GSL. This approach allows us to quantitatively compare acoustic and visual surveys to better inform future right whale risk reduction options.

2 | METHODS

2.1 | Survey domains

Domains were created to approximate the representative dynamic management DFO fishing zones and TC speed restriction zones from the 2020 management plan for the GSL. A DFO domain was modeled to be 18 km tall by 12 km wide, while a TC domain was modeled to be 20 km tall by 100 km wide (Johnson et al., 2021; Figure 1). We consider the width of a survey domain to be its length from West–East. Each domain was centered at 0 on a Cartesian grid in the model.

2.2 | Whale model

An autocorrelated random walk was used to simulate the movement of whales engaged in feeding behavior.

Feeding behavior was chosen as there is evidence of right whales feeding in the GSL habitat and it represents an intermediate spatial and behavioral scale between traveling and socializing (Johnson et al., 2020). The model began by placing a whale at a given location, then assigned speeds and turning angles at regular timesteps (2.5 s) for the duration of the simulation. The initial direction of whale movement was selected randomly from a uniform distribution of angles between 0° and 360°. Subsequent turning angles were chosen from a uniform distribution between the minimum and maximum turning angles for a whale moving while in the feeding behavior, or -19.3° and $+19.3^\circ$ degrees per decameter (Johnson et al., 2020). For swimming speed, values were chosen at random at each simulation timestep from a uniform distribution of speeds between 0 and 1.23 m s^{-1} , as previously obtained from satellite radio tags on right whales in their feeding habitats (Baumgartner & Mate, 2005). More details of the movement model are described in Johnson et al. (2020). Initial whale position was assigned randomly within the survey domain. The whales were reflected at the boundaries of the DFO and TC domains to retain them within the domain for the duration of the transit by the survey platform. When a whale was reflected at the boundary, the whale path incident and reflected angles were equal.

To assess the detection capabilities of the different platforms, production of calls and dive cycles were added to the model whale using distributions of dive times and calling rates based upon best-available observations. The dive cycle comprised of a dive interval defined as a normal distribution with a mean dive time of 720 s (12 min) and a standard deviation of 180 s (3 min), and a surface interval defined as a normal distribution with a mean surface time of 300 s (5 min) and a standard deviation of 60 s (1 min; Baumgartner & Mate, 2003). The initial dive state was determined by drawing from a binomial distribution using the probability of a whale being underwater at any moment (mean dive time divided by total cycle duration, or $720 \text{ s} / [720 \text{ s} + 300 \text{ s}] = 0.71$). Following initialization, the whale dive state alternated from being at depth or at the surface, with the duration of each state drawn from the above dive cycle distributions.

Calling rates were modeled as upcall production, as upcalls are well-documented contact calls (e.g., Parks & Tyack, 2005) used by PAM systems, both real-time and archival, to determine right whale presence in an area (e.g., Baumgartner et al., 2017; Davis et al., 2017). Franklin et al. (2022) studied right whale calling behavior in whale aggregations (≥ 3 whales) with respect to time and observed behavior (i.e., foraging and socializing) using sonobuoys in the GSL from June to August in 2017, 2018, and 2019. Their upcall production rate was derived from

counting the number of upcalls per audio recording duration per number of whales seen within that recording duration (upcalls $\text{h}^{-1} \text{ whale}^{-1}$). To avoid further assumptions about the under-studied phenomenon that is right whale calling, we fit various types of distributions (uniform, normal, exponential, and logistical) to Franklin et al.'s right whale upcall production rates and, using packages “fitdistrplus” (Delignette-Muller & Dutang, 2015) and “AICcmodavg” (Mazerolle, 2020), compared the different distributions to find that which best resembled their observations. While none of the four different types of distributions altered the results, the exponential distribution best fit their observed data, which had a high probability of a zero-calling rate (Franklin et al., 2022). The exponential distribution had a rate of 4.272 and was truncated to a maximum calling rate of 2 upcalls $\text{h}^{-1} \text{ whale}^{-1}$ to account for outliers. Values from the exponential distribution were assigned to each model timestep to determine the probability of a whale calling. These probabilities were entered into a binomial distribution to determine the calling state of a whale in each timestep.

2.3 | Survey platforms

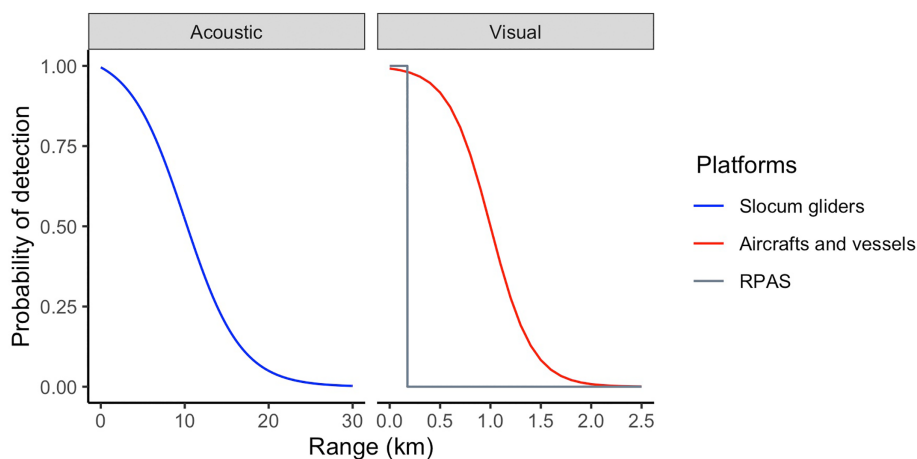
To create the tracks for survey transits through each domain by each platform, nominal speeds for each were fixed with random start and end points on the left (West) and right (East) sides of the domain, respectively. Aircrafts, RPAS, vessels, and Slocum gliders were included in the simulation. Aircrafts transited at 51 m s^{-1} (100 knots), RPAS at 41.2 m s^{-1} (80 knots), vessels at 4 m s^{-1} (8 knots), and Slocum gliders at 0.1 m s^{-1} (0.2 knots). The model interpolated the positions of each platform between start and end positions to create tracks running the width of the survey domain from West to East, as is typical of GSL surveys (Johnson et al., 2021), with the same time resolution as the simulated whales.

Detection functions were assigned to each platform and defined as the probability of detecting a whale as function of range. The detection functions for the aircraft, vessel, and Slocum glider were defined using a logistic curve, $y = L / (1 + e^{-k \cdot [x - x_0]})$, where y is the probability of detection, L is the maximum y value, k is the logistic growth rate, x_0 is the value or distance at the midpoint of the curve (0.5 detection probability), and x is any distance from the whale cue (Table 1). We set a 0.5 probability of an aircraft or vessel detecting a whale at the surface at 1.5 km (Ganley et al., 2019; Williams et al., 2016) and a 0.5 probability of a Slocum glider detection of a whale call at 10 km (Johnson et al., 2022; Table 1). The RPAS detection function was defined by a 1.0 probability of

TABLE 1 Summary information (nominal speed, average time spent in the DFO and TC survey domains, cost of deployment, total detection range, detection range at 0.5 detection probability, detection function parameters, and associated sources) for the aircraft, RPAS, vessel, and Slocum glider platforms

| | Aircraft | RPAS | Vessel | Slocum glider |
|------------------------------------|---|---|---|---|
| Speed (knots) | 100 | 80 | 8 | 0.2 |
| Speed (m s ⁻¹) | 51 | 41.2 | 4 | 0.1 |
| Δt in domains (mins) | 5 (DFO) 30 (TC) | 6 (DFO) 40 (TC) | 60 (DFO) 402 (TC) | 2340 (DFO) 16,740 (TC) |
| Cost of deployment (CAD/h) | 1592 | NA | 700 | 31.25 |
| Detection range (km) | 1.9 | 0.172 | 1.9 | 20 |
| Range at 0.5 detection probability | 1.5 | 0.172 | 1.5 | 10 |
| Detection function | $P(x) = L/(1 + e^{-k*[x-x_0]})$ | $P(x) = \{1 \text{ for } x \leq 0.175, \text{ } 0 \text{ for } x > 0.175\}$ | $P(x) = L/(1 + e^{-k*[x-x_0]})$ | $P(x) = L/(1 + e^{-k*[x-x_0]})$ |
| Detection function parameters | $L = 1$ $k = -4.8$ $x_0 = 1$ | NA | $L = 1$ $k = -4.8$ $x_0 = 1$ | $L = 1.045$ $k = -0.3$ $x_0 = 10$ |
| Detection function sources | Williams et al., 2016; Ganley et al., 2019 | M. McKeeman, personal communications, April 23, 2021 | Williams et al., 2016; Ganley et al., 2019 | Johnson et al., 2022 |

FIGURE 2 Probability of detection functions by range (in kilometers) for the aircraft and vessel (red), RPAS (gray), and Slocum glider (blue). Note the different in x -axis scales for the acoustic and visual platforms. Detection function parameters are available in Table 1



detecting a whale in the RPAS visual field, which was a radius of ~ 172 m, and a detection probability of 0 beyond that range (M. McKeeman, personal communication, April 23, 2021; Table 1).

These functions were used to determine the probability that a whale cue would be detected as a function of range to the survey platform (Figure 2). Factors other than range affecting detection probability (e.g., sea state, ambient noise, etc.) were not considered in these functions; the equations do not depend on changing weather and behave as if survey conditions are good. This detection probability was computed for every surfacing or call and entered in a binomial distribution to determine if a

whale was detected or not. The resulting detections were then modified for visual platforms to ensure that these were counted on a per-surfacing basis, that is, multiple detections of a single whale at the surface were recorded as a single detection.

2.4 | Survey simulation

A single model run was defined as a single transit by each of the four platforms in a given domain with a given number of whales (also referred to as “whale number”; Figure 3). We chose to use the following

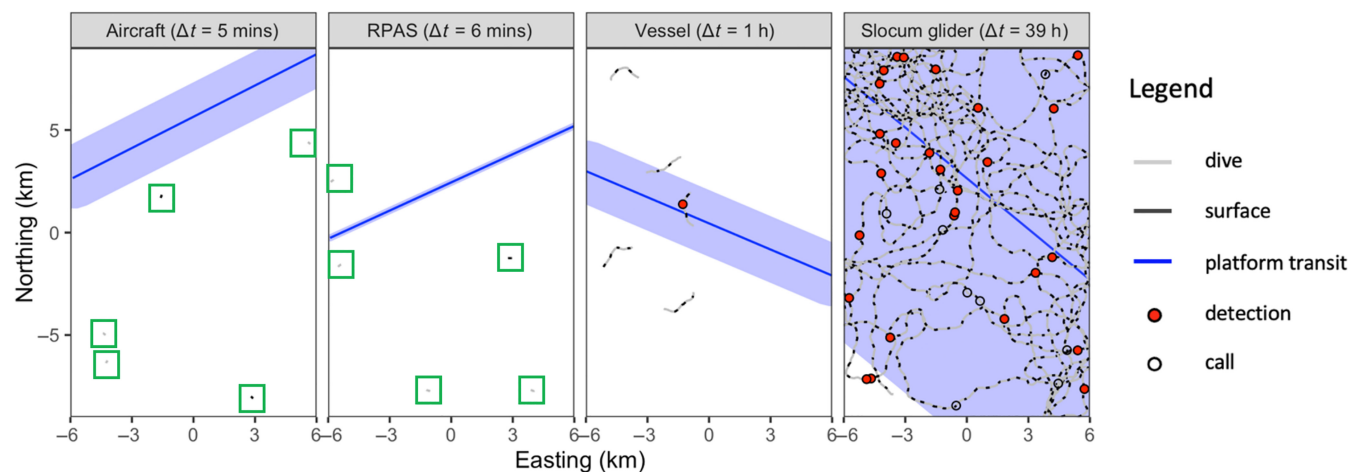


FIGURE 3 Example of one simulation run in a DFO domain for each survey platform and five whales, including platform transit (dark blue) and area of 0.5 probability of detection (light blue), diving whale (gray segments), whale at surface (black segments), whale calls (black circles), and visual and acoustic detections for each platform (red circles). Platform type and the approximate transit time (Δt) is shown in each panel label. Green boxes highlight whale positions in the aircraft and RPAS panels

whale numbers: low concentrations (range 1–10, increment 1) and high concentrations (range 15–100, increment 5). The low concentrations are based on typical observations from 100 of surveys over the years, and while 65 whales is the largest number reported in a DFO fisheries grid cell in the southern GSL (Johnson et al., 2021), we expanded the maximum range to 100 whales to resolve platform performance at extremely high whale concentrations. The high concentration increment of five whales was used to reduce computational demands.

The Monte Carlo approach that made up our simulation consisted of 224 different combinations of platform, whale number, and domain-type, each run 10,000 times. We expected to have 2,240,000 total transits in the simulation. Running the model more than 10,000 times did not affect the simulation results, suggesting that 10,000 replicates was sufficient to represent the uncertainty of the estimates. During model development, it became clear that Slocum glider transits always detected whales, so we decreased the number of transits for Slocum gliders when the whale number exceeded 10 to reduce computational demand. This had no impact on the results. The probability of detecting at least one whale on one transit, $P_T(1)$, was defined as the proportion of all the runs for that particular combination of platform type and whale number with detections (i.e., the total number of transits with at least one detection divided by the total number of transits). The probability of detecting at least one whale on n transits was calculated using $P_T(n) = 1 - (1 - P_T(1))^n$, which assumes transits are independent.

2.5 | Platform performance metrics

To further evaluate the effectiveness of each platform in the model, performance metrics were calculated. Specifically, for each combination of platform and whale number in both domains, the number of transits, time (h), and the cost (Canadian dollars) required to achieve a detection probability of 0.5 and 0.95 were calculated (referred to as $N_{0.5}$, $T_{0.5}$, and $C_{0.5}$, and $N_{0.95}$, $T_{0.95}$, and $C_{0.95}$, respectively). We included the 0.5 and 0.95 detection probability scenarios to represent monitoring that is tolerant and adverse to the risk of missing right whales. $N_{0.5}$ and $N_{0.95}$ for each combination was determined by selecting the number of transits which best approximated an absolute $P_T(n)$ value of 0.5 and 0.95, respectively. $T_{0.5}$ and $T_{0.95}$ were found by multiplying $N_{0.5}$ and $N_{0.95}$ values for each combination, respectively, by their average transit time in each domain (Table 1). $C_{0.5}$ and $C_{0.95}$ were found by multiplying $T_{0.5}$ and $T_{0.95}$ values for each combination, respectively, using nominal estimates of their hourly survey costs in each domain (Table 1). The RPAS platform is still in active development and operational cost estimates remain unknown.

The simulation was implemented using R version 3.6.3 (R Core Team, 2020). Data analyses used utilities from the “tidyverse” (Wickham et al., 2019), “lubridate” (Grolemund & Wickham, 2011), “zoo” (Zeileis & Grothendieck, 2005), “sp” (Pebesma & Bivand, 2005), “rgeos” (Bivand & Rundel, 2020), and “raster” (Hijmans, 2020) packages. Data visualization used the “ggplot2” (Wickham, 2016), “sf” (Pebesma, 2018), “maptools” (Bivand & Lewin-Koh, 2019), and “ggspatial” (Dunnington, 2021) packages. Charting the GSL and

DFO and TC areas was recreated using the “rnaturalrth” (South, 2017) package and bathymetric data (“ETOPO1,” NOAA, 2009). All code required to reproduce the simulation and result analyses is available at https://github.com/hansenjohnson/detection_sim.

3 | RESULTS

The survey transits by the Slocum glider were of greater duration than those of the visual survey platforms. On an average transit, aircrafts and RPAS spent ~ 5 min in the DFO domain and 30–40 min in the TC domain, and vessels spent ~ 1 h in the DFO domain and nearly 7 h in the TC domain. In contrast, the Slocum glider spent on average nearly 39 h in the DFO domain and almost 279 h in the TC domain (Table 1).

The probability of detecting at least one whale on a single transit, $P_T(1)$, depended primarily on the platform used and the whale number in an area. Aircrafts required ~ 20 whales to achieve a $P_T(1)$ of 0.5 in either domain (i.e., a 1 in 2 chance of detection). A $P_T(1)$ of 1.0 was approached (maximum $P_T(1)$ reached was ~ 0.95) but not achieved with the maximum 100 whales simulated in either domain, meaning there was a small chance (~ 0.05) that an aircraft would fail to detect at least 1 of 100 whales on a single transit. The RPAS achieved a maximum $P_T(1)$ of ~ 0.25 with 100 whales in either domain,

meaning there was a 1 in 4 chance of detecting at least 1 of 100 whales on a single transit. For vessels, a $P_T(1)$ of 0.5 required ~ 3 whales and a $P_T(1)$ of 1.0 required ~ 30 whales in either domain. Slocum gliders always detected a whale on a single transit regardless of the whale number or the domain in which the survey was conducted (i.e., $P_T(1)$ was always 1.0; Figure 4a).

The probability of detecting a whale also depended on the number of transits performed by each platform. If there was only one whale present, aircrafts required ~ 20 transits to achieve a $P_T(n)$ of 0.5, or over 100 transits to approach a $P_T(n)$ of 1.0 in either domain (Figure 4b). The performance of the RPAS varied slightly between management domains. If only a single whale was present, the RPAS reached a maximum $P_T(n)$ of ~ 0.2 in the DFO domain and ~ 0.25 in the TC domain with 100 transits. Vessels needed ~ 3 transits to achieve $P_T(n) = 0.5$, or ~ 25 transits for $P_T(n) = 1.0$ for a single whale in either domain. Slocum gliders always detected a whale, no matter the number of transits or the survey domain (i.e., $P_T(n)$ was always 1.0). If both whale number and the number of transits increased, $P_T(n)$ for aircrafts, RPAS, and vessels rose rapidly (Figure 4b).

The various performance metrics facilitated more subtle comparisons among platforms. Increasing whale number decreased the values of $N_{0.5}$, $T_{0.5}$, $C_{0.5}$, $N_{0.95}$, $T_{0.95}$, and $C_{0.95}$ for all platforms except Slocum gliders, where the performance metric values were constant

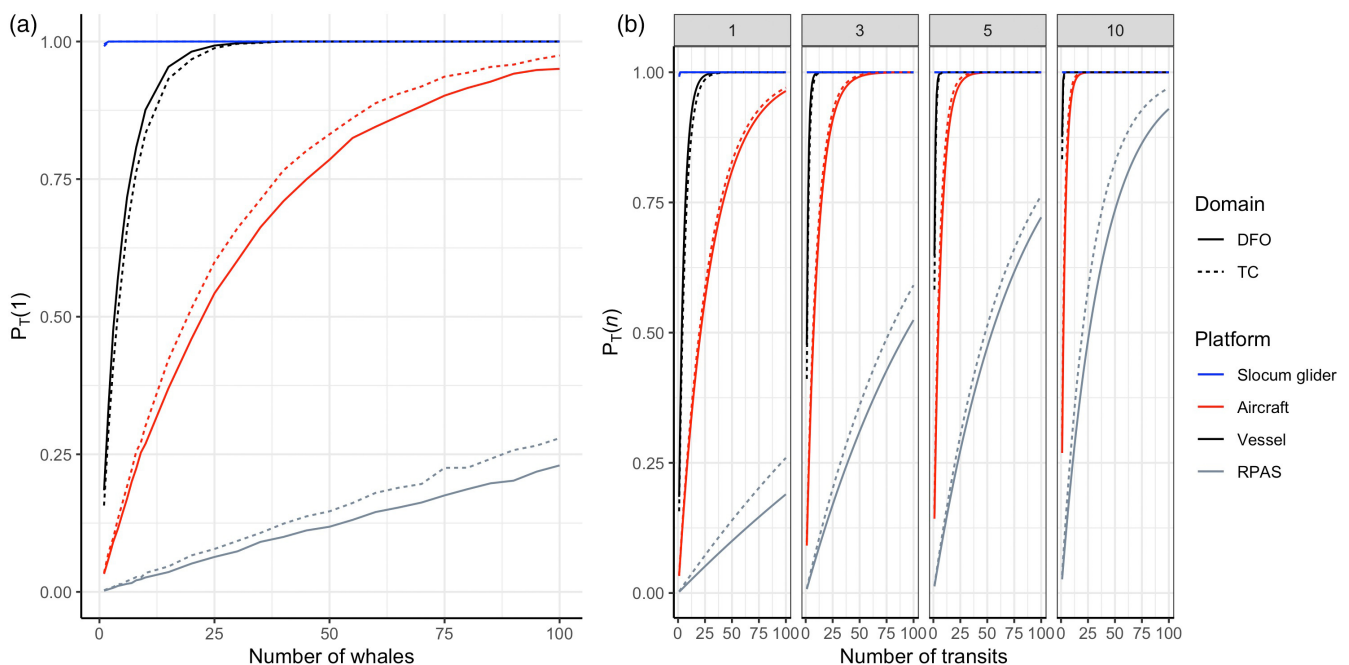


FIGURE 4 Probability of detecting at least one whale from a Slocum glider (blue), aircraft (red), vessel (black) or RPAS (gray) in a DFO (solid line) or TC (dashed line) dynamic management domain. Left panel (a) shows results for a single survey transit, $P_T(1)$, and 1–100 whales. Right panel (b) shows results with 1–100 transits, $P_T(n)$, over multiple (1, 3, 5, or 10) whales (shown in each panel)

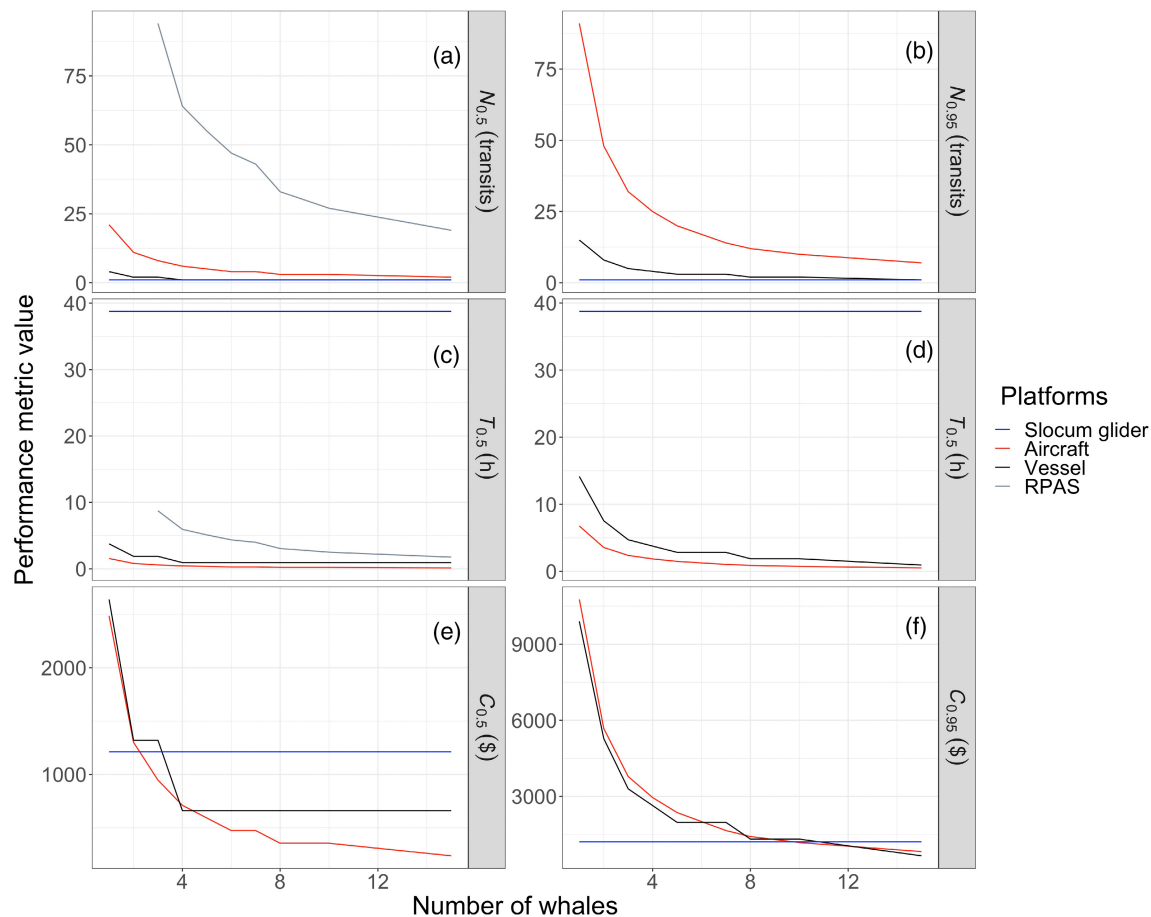


FIGURE 5 Performance metrics representing the number of transits (N), time (T ; hours), and cost (C ; Canadian dollars) required to achieve a detection probability of 0.5 (left column) and 0.95 (right column) for all four platforms (aircraft, RPAS, vessel, and Slocum glider) with increasing whale numbers (1–15) in the DFO dynamic management domain. Note the difference in y-axis scales among panels

across all numbers of whales (Figure 5). Much like the $P_T(n)$ results, when whale number was high (>10 whales in a DFO domain), all platforms required 1 or, at most for the aircraft, 2 transits to achieve a detection probability of 0.5 ($N_{0.5}$), except for the RPAS, which always had higher $N_{0.5}$ values (Figure 5a). When whale number was low (<15), aircrafts and vessels always required more transits to achieve a detection probability of 0.95 ($N_{0.95}$) versus 0.5 (Figure 5b). Variations in the time required to detect whales with a probability of 0.5 ($T_{0.5}$) and 0.95 ($T_{0.95}$) were driven primarily by platform speed, with visual platforms taking much less time than the acoustic platform (typically <5 h for visual versus ~ 39 h for acoustic in a DFO domain; Figure 5). Note that, because the RPAS only reached a detection probability ≥ 0.5 and ≥ 0.95 when ≥ 3 and ≥ 15 whales were present, respectively, some values for $N_{0.5}$, $T_{0.5}$, $N_{0.95}$, and $T_{0.95}$ could not be calculated (Figure 5). Costs required to detect whales with a probability of 0.5 ($C_{0.5}$) and 0.95 ($C_{0.95}$) depended on the number of whales and platform. At the 0.5 probability level, aircrafts were only consistently more cost-

effective than vessels when whale number was >4 (Figure 5e). For the detection probability range of 0.5–0.95, the cost to detect a single right whale in a DFO domain was $\sim \$2500$ – $\sim \$10,800$ for aircrafts, or $\sim \$2600$ – $\sim \$9900$ for vessels (Figure 5). The cost of visual surveys dropped as the number of whales increased. Detecting a right whale acoustically within a survey domain always cost $\$1200$ (i.e., the cost of a single transit), regardless of the number of whales. At the 0.95 probability level, aircrafts and vessels became more cost effective than Slocum gliders when >10 whales were present (Figure 5). Trends were consistent between domains, with $T_{0.5}$, $C_{0.5}$, $T_{0.95}$, and $C_{0.95}$ having values 6–10-fold greater in a TC domain (not shown).

4 | DISCUSSION

Factors such as the nature of the cues being detected, platform detection range, and monitoring persistence affect the probability of detection for visual and acoustic

surveys. In our simulation, Slocum gliders always acoustically detected right whales in a single transit of a management domain, regardless of the number of whales, while visual surveys required multiple whales and/or numerous transits to reliably (>0.5 detection probability) detect right whale presence. This demonstrates that the increased detection range and monitoring persistence of acoustic platforms more than compensate for the infrequent and variable calling rate of right whales. Previous studies comparing visual and acoustic surveys in the field documented similar results. Clark et al. (2010) concluded that acoustics provide a more reliable option than aerial surveys for detecting right whale presence in Cape Cod Bay, as aerial surveys in the region detected whales on only two-thirds of the days that the acoustic surveys did over approximately 2 months. Similarly, for Durette-Morin et al. (2019), vessel surveys in Roseway Basin recorded lower right whale presence overall than archival PAM surveys. Their results also indicated that relying solely on visual surveys may lead to erroneous conclusions about trends in habitat occupation, as visual data implied a decline in right whale presence from 2014 to 2015 in Roseway Basin relative to 2004–2005, but acoustic data did not demonstrate such a trend (Durette-Morin et al., 2019).

Although all management measures in the GSL are triggered by the detection of a single right whale, the odds of sighting a single right whale on a single transit (with good visual conditions) with the simulation were very low (<0.1 for an aircraft, <0.05 for a RPAS, and <0.2 for a vessel). Thus, we conclude that single transits by visual surveys cannot reliably detect single right whales in DFO or TC management zones, and as such cannot be used to confidently rule out right whale presence. This result is intuitive, as an aircraft traveling at typical survey speeds ($\sim 51 \text{ m s}^{-1}$) will complete a West–East transit of a simulated DFO management domain ($\sim 12 \text{ km}$) in under 5 min, or less than half of the duration of a typical right whale foraging dive ($\sim 12 \text{ min}$; Baumgartner & Mate, 2003). In contrast, an acoustic Slocum glider will always detect single whales (if the whale is calling), because it completes a survey transit of a simulated DFO domain in $\sim 39 \text{ h}$. During this time, since the range to a detection probability of 0.5 for a Slocum glider is 10 km, it is monitoring nearly the entire DFO management zone. In summary, effective detection and risk management of single whales requires multiple visual survey transits, increased reliance on acoustic platforms, alternative technologies, or some combination thereof.

Due to the low odds of visually detecting a single whale, when right whales are sighted on single transits of a management zone it is very likely that there are additional whales in the vicinity, as a >0.5 detection

probability during one aircraft transit in the simulation occurs when >10 whales are present. This is qualitatively consistent with the observed distribution of right whales within the GSL in recent years, as most sightings are clustered in the Shediac Valley region of the southern GSL where right whales are known to aggregate in large numbers. Aggregations are also often observed north of Anticosti Island. Right whales traveling between these areas must transit the TC dynamic shipping zones. Weekly aerial surveys of these zones have detected very few right whales, but Slocum glider-based acoustic monitoring in 2020 and 2021 detected persistent whale presence (Johnson et al., 2021).

There were also substantial differences in performance among visual survey platforms. Vessels, for instance, performed better than either the aircraft or RPAS. This was a result of their increased persistence in a survey domain, as the only difference between vessels and aircrafts in the simulation was the platform speed. Traveling slower and spending additional time in a domain allowed a vessel to detect more cues. The RPAS and aircraft traveled at similar speeds, so the relatively poor performance of the RPAS was driven by its limited detection range, which was nearly an order of magnitude smaller than that of the vessel or aircraft. The RPAS is still being actively developed as a monitoring platform, but it currently does not provide a reliable means of detecting right whale presence, even with many transits over many whales. RPAS performance may improve substantially by increasing the system detection range, and, to a lesser extent, by reducing the transit speed. Once operational, a potential benefit of the RPAS as an autonomous platform would be the ability to scale up monitoring effort by deploying multiple platforms.

Decision-makers can use our combined model approach and simulation results as tools to develop more informed monitoring plans that capitalize on the relative strengths and weaknesses of each platform and can then tailor those plans to desired risk tolerance levels. For example, consider a group of 10 right whales in a DFO zone. Our results suggest that detecting at least one of the 10 individuals with 50% certainty (0.5 detection probability) would require three transits by an aircraft ($\sim \$350$), one transit by a vessel ($\sim \$660$), and one transit by a Slocum glider ($\sim \$1200$) or, to obtain 95% certainty (0.95 detection probability), 10 by an aircraft ($\sim \$1200$), two by a vessel ($\sim \1300), and one by a Slocum glider ($\sim \$1200$). Within the same domain, detecting a single right whale feeding alone with 50% certainty would require 20 transits by an aircraft ($\sim \$2500$), four transits by a vessel ($\sim \$2600$), and one transit by a Slocum glider ($\sim \$1200$), or, to obtain 95% certainty, 90 by an aircraft ($\sim \$10,700$), 15 by a vessel ($\sim \9900), and one by a Slocum glider

(~\$1200). These examples and our results apply to the monitoring of a single dynamic management zone. Scaling up the efforts needed to detect a single right whale with 95% certainty to cover the entirety of the southern GSL, which contains approximately 200 of these DFO zones, is a more conservative management scenario that would require approximately 1500 h (~\$2.1 M) of aircraft surveillance, 3000 h (~\$2 M) of vessel surveillance, and 7800 h (~\$240,000) of Slocum glider surveillance. This simple exercise does not address the logistics of site-specific survey implementations or the associated economic constraints, such as compensating operators, maintaining platforms, or traveling to the management zone in question, as these are beyond the scope of our work. Instead, we provide a minimum estimate and generic description of the order of magnitude between platform costs, demonstrating how our approach can help compare different surveys and management goals from a cost-effective perspective.

Despite being based on several assumptions, agent-based models such as the one used here often have important ramifications for species management and have proven useful for cetacean management particularly (e.g., Chion et al., 2017). The flexibility of the simulation-based approach allows adaptations to address many right whale-related scientific or conservation objectives in the future. Previous right whale modeling work demonstrated that lethal vessel strikes decrease with voluntary compliance in a designated Area To Be Avoided in Roseway Basin (van der Hoop et al., 2012) and that whale location uncertainties following a detection vary with whale behavior and detection ranges, but become equivalent within 2 days for both visual and acoustic detections (Johnson et al., 2020). The current version of our model could be useful for the assessment of specific monitoring tools and management strategies such as the optimization of platform survey plans. For Slocum gliders, these have been evaluated empirically in the past to maximize management zone coverage and probability of right whale encounter (Durette-Morin, 2021), but it would be informative to use a simulation-based approach such as ours to quantitatively compare survey designs. Our simulation could also be used to evaluate the potential of other methodologies and platforms being developed for right whale monitoring, such as satellite imagery (e.g., Bamford et al., 2020), thermal imaging-based detection systems (e.g., Zitterbart et al., 2020), or autonomous surface vehicles (“wave gliders”) that are not yet as effective at PAM as other well-characterized platforms (e.g., Baumgartner et al., 2021). Furthermore, if movement and acoustic behavior of the species is known, this approach can be adapted to improve conservation outcomes for other species. We support these and other

expansions of this work by making the source code for our analyses openly available.

4.1 | Assumptions and caveats

We did not consider ancillary data collection by visual surveys in our comparison of survey platforms. Rather, our goal was to provide a means to directly compare the cue-detecting performance of the different survey platforms used for near real-time right whale monitoring. To do so, we developed and parameterized the model simulation based upon the best available information, and in some cases relied upon several simplifying assumptions. For instance, we incorporated the only available information on calling rates for right whales in their GSL feeding grounds during summer as defined by Franklin et al. (2022). Among other results, Franklin et al. (2022) found that right whale foraging behaviors negatively correlated with upcalls and ultimately reported a median of 0.2 upcalls h^{-1} whale $^{-1}$. The estimated call production rate for North Atlantic right whales found by Matthews et al. (2001) in the Gulf of Maine was 1.743 moans whale $^{-1}$ $\text{h}^{-1} \pm 27\%$ CV (as presented in Marques et al., 2011), which is slightly higher than the range of observations by Franklin et al. (2022). Note that Matthews et al. (2001) used a broad call classification “moan” for right whale vocalizations which included upcalls along with other right whale calls. Higher or lower calling rates would theoretically decrease or increase availability bias, respectively, for acoustic surveys and affect the total detections by Slocum gliders. We chose to use the estimate from Franklin et al. (2022) to parameterize whale calling rate because their rate was more conservative, the study site matched that of this study, and upcalls, not moans, are typically used in passive acoustic monitoring to determine right whale presence (e.g., Davis et al., 2017).

Though we included large numbers of right whales in the simulation, whales were distributed randomly within a management domain and the behavior of each whale was independent (i.e., was not influenced by the presence of other whales). We made no attempt to incorporate changes in movement, calling, or diving that likely arise from group- or density-specific behaviors. In the field, right whales are often observed in surface active groups (SAGs), defined as groups of two or more right whales interacting at the surface (e.g., Parks et al., 2007). While their composition may vary, SAGs are characterized by prolonged periods of surface displays, thus their probability of detection by visual surveys will likely increase since availability biases are reduced. As for acoustic cues, previous findings show that right whale upcall rates increase

with socialization (Franklin et al., 2022) and in SAGs (Parks & Tyack, 2005). There are areas of the southern GSL where right whales are known to gather in SAGs within DFO management zones (Johnson et al., 2021), but for the sake of simplicity we made no attempt to incorporate this into our simulation. This assumption could potentially have reduced the total number of visual and acoustic cues available to our survey platforms at high whale abundances, which would cause our simulation to underestimate performance of both visual and acoustic surveys.

The whales in our simulation use solely one behavior and remain within one survey domain for extended periods. They also perform the same behavior in both simulation domains. These constraints were necessary to directly compare platform performances within and between survey domains. Though we suspect that maintaining a specific behavior on timescales like those of our simulated Slocum glider transits (39–280 h) is unlikely for right whales, there is no available information on their behavioral budgets. Right whale behavior is potentially associated with management zone type, as there is little evidence suggesting formation of large aggregations such as the ones in our simulation in TC zones (Johnson et al., 2021), but the exact way right whales are using these different areas is poorly known. It is thought that diving during foraging depends on factors such as the vertical distribution of copepod prey, and that right whales change their diving frequency and duration accordingly (Baumgartner et al., 2017). Our simulation dive cycle parameters are based on data from time-depth-recorders attached to right whale individuals in the Bay of Fundy and Roseway Basin (Baumgartner & Mate, 2003) and therefore include fine-scale variability in behavior while feeding within a habitat. We attempt to account for changes in swimming and surfacing through our modeled parameters and assume the Bay of Fundy data are representative of typical foraging dive times in the southern GSL, but we made no effort to incorporate additional unknown variability for other locations, such as the TC domain. Choosing a different behavior for the whales in our simulation model would mean changing calling and diving rates accordingly, possibly affecting platform performance.

Another important assumption we made was that aircrafts and vessels have the same detection function. Williams et al. (2016) report detection probability curves aboard vessels for humpback whales that are nearly identical to those published by Ganley et al. (2019) aboard aircrafts for right whales. These two studies examined different species with different methodologies and arrived at nearly identical results, hence the use of the same detection probability curves for these two visual platforms in our simulation. However, considering the range

of conditions and types of surveys that both platforms must conduct, it is possible that aircrafts and vessels have different detection capabilities. In addition, our simulation assigns a constant probability of detection throughout the entire surfacing interval, while in reality whales are typically only visible over several short intervals during that period. This means that we are likely overestimating the performance of traditional visual platforms (aircrafts and vessels). There is some evidence that RPAS can detect whales subsurface (M. McKeeman, personal communication, April 23, 2021), in which case the simulated performance of this platform is less biased. For simplicity's sake, different weather conditions were not modeled, and the detection functions of all platforms are constant throughout the simulation, which is perhaps not representative of a typical right whale monitoring season in the GSL. Thus, a lot of variability can stem from modeling different detection functions unique to each platform's typical survey style and type.

For simplicity purposes, we excluded static surveys (such as visual observations from the coast or acoustic detections from moored buoys) from the simulation, as they cannot perform transits over an area, like moving aircrafts, vessels, RPAS, and Slocum gliders can. Since we have found that time spent in a domain largely affects the whale-detecting performance of a platform, it is difficult to compare how a stationary PAM platform, such as a moored buoy outfitted with an acoustic receiver, might perform next to a Slocum glider. In theory, the detection range of the static hydrophone would encompass the majority of a DFO domain in a simulation, and only a minority of a TC domain, which would likely result in different detection probabilities reflecting this monitoring effort. We also assume that all platform track lines are perfectly straight and always randomly transit a domain from left-to-right. Since our simulation does not include any deviations from this straight track line, it cannot account for subsequent detections when circling an area after an initial detection, a common practice for both vessel and aircraft surveys. Including these changes would possibly increase total detections but would not improve initial whale detectability or presence estimates for risk management purposes. Additionally, we made no attempt to apply a systematic survey design within a transit area. Since survey designs are different in shape and duration among the four platforms used in our simulation, our random left-to-right survey methodology presented the simplest option for comparison between visual and acoustic surveys. Changing platform track lines according to real survey designs may lead to results that are more representative of what is occurring in a certain management area at a certain time but would make it more difficult to compare among platforms.

4.2 | Conclusions

Acoustic surveys by Slocum gliders provide more reliable estimates of right whale presence than visual surveys by aircraft, RPAS, and vessels in dynamic risk management zones, especially for detecting few right whales. This is due in part to the increased persistence and detection range of acoustic platforms. Single transits of a management zone by visual surveys were not able to reliably (>0.5 probability) detect single right whales and therefore cannot be used to confidently rule out right whale presence within a management zone. This agrees well with the observed distribution of right whales in Canadian waters, with the vast majority of sightings occurring in areas where right whales aggregate and few sightings of whales traveling among other areas. Our methods and results provide a tool that can be used to design more efficient and effective dynamic management and monitoring strategies that take advantage of the relative benefits of each survey platform.

AUTHOR CONTRIBUTIONS

Valentina Ceballos, Hansen Johnson, and Christopher Taggart conceived of and designed the study. Valentina Ceballos and Hansen Johnson conducted the analysis. Valentina Ceballos drafted the initial manuscript. All authors contributed to the review and submission of the final manuscript.

ACKNOWLEDGMENTS

We owe many thanks to Delphine Durette-Morin, Kimberly Franklin, Mark Baumgartner, Angelia Vanderlaan, Gina Lonati, Moira Brown, Sean Brilliant, Mark McKee-man, and others in the right whale research community for helpful feedback and discussions. Valentina Ceballos was supported by the Nancy Witherspoon Memorial Summer Research Award and the Rob Stewart Award in Marine Conservation from Dalhousie University. Hansen Johnson was supported by a Vanier Canada Graduate Fellowship, Killam Predoctoral Scholarship, Nova Scotia Graduate Research Scholarship, and Dalhousie University President's Award.

CONFLICT OF INTEREST

The authors have no conflicts of interest to declare.

DATA AVAILABILITY STATEMENT

All code required to reproduce this simulation and analysis is available at:

https://github.com/hansenjohnson/detection_sim.

ETHICS STATEMENT

Not applicable.

ORCID

Valentina Ceballos  <https://orcid.org/0000-0002-6354-5679>

Hansen Johnson  <https://orcid.org/0000-0002-3086-6759>

REFERENCES

- Bamford, C. C. G., Kelly, N., Dalla Rosa, L., Cade, D. E., Fretwell, P. T., Trathan, P. N., Cubaynes, H. C., Mesquita, A. F. C., Gerrish, L., Friedlaender, A. S., & Jackson, J. A. (2020). A comparison of baleen whale density estimates derived from overlapping satellite imagery and a shipborne survey. *Scientific Reports*, *10*, 12985.
- Baumgartner, M., Cole, T., Clapham, P., & Mate, B. (2003). North Atlantic right whale habitat in the lower Bay of Fundy and on the SW Scotian Shelf during 1999–2001. *Marine Ecology Progress Series*, *264*, 137–154. <https://doi.org/10.3354/meps264137>
- Baumgartner, M. F., Ball, K., Partan, J., Pelletier, L.-P., Bonnell, J., Hotchkin, C., Corkeron, P. J., & van Parijs, S. M. (2021). Near real-time detection of low-frequency baleen whale calls from an autonomous surface vehicle: Implementation, evaluation, and remaining challenges. *The Journal of the Acoustical Society of America*, *149*, 2950–2962.
- Baumgartner, M. F., Bonnell, J., Corkeron, P. J., Van Parijs, S. M., Hotchkin, C., Hodges, B. A., Thornton, J. B., Mensi, B. L., & Bruner, S. M. (2020). Slocum gliders provide accurate near real-time estimates of baleen whale presence from human-reviewed passive acoustic detection information. *Frontiers in Marine Science*, *7*, 100. <https://doi.org/10.3389/fmars.2020.00100>
- Baumgartner, M. F., & Mate, B. R. (2003). Summertime foraging ecology of North Atlantic right whales. *Marine Ecology Progress Series*, *264*, 123–135. <https://doi.org/10.3354/meps264123>
- Baumgartner, M. F., & Mate, B. R. (2005). Summer and fall habitat of North Atlantic right whales (*Eubalaena glacialis*) inferred from satellite telemetry. *Canadian Journal of Fisheries and Aquatic Sciences*, *62*, 527–543. <https://doi.org/10.1139/F04-238>
- Baumgartner, M. F., Wenzel, F., Lysiak, N., & Patrician, M. (2017). North Atlantic right whale foraging ecology and its role in human-caused mortality. *Marine Ecology Progress Series*, *581*, 165–181. <https://doi.org/10.3354/meps12315>
- Bivand, R., & Lewin-Koh, N. (2019). mapproj: Tools for handling spatial objects. R package version 0.9-9. Retrieved from <https://CRAN.R-project.org/package=mapproj>
- Bivand, R., & Rundel, C. (2020). rgeos: Interface to geometry engine—open source ('GEOS'). R package version 0.5-5. Retrieved from <https://CRAN.R-project.org/package=rgeos>
- Chion, C., Lagrois, D., Dupras, J., Turgeon, S., McQuinn, I. H., Michaud, R., Ménard, N., & Parrott, L. (2017). Underwater acoustic impacts of shipping management measures: Results from a social-ecological model of boat and whale movements in the St. Lawrence River estuary (Canada). *Ecological Modelling*, *354*, 72–87. <https://doi.org/10.1016/j.ecolmodel.2017.03.014>
- Clark, C. W., Brown, M. W., & Corkeron, P. (2010). Visual and acoustic surveys for North Atlantic right whales, *Eubalaena glacialis*, in Cape Cod Bay, Massachusetts, 2001–2005: Management implications. *Marine Mammal Science*, *26*(4), 837–854. <https://doi.org/10.1111/j.1748-7692.2010.00376.x>
- Davies, K. T. A., & Brilliant, S. W. (2019). Mass human-caused mortality spurs federal action to protect endangered North Atlantic

- right whales in Canada. *Marine Policy*, 104, 157–162. <https://doi.org/10.1016/j.marpol.2019.02.019>
- Davis, G. E., Baumgartner, M. F., Bonnell, J. M., Bell, J., Berchok, C., Thornton, J. B., Brault, S., Buchanan, G., Charif, R. A., Cholewiak, D., Clark, C. W., Corkeron, P., Delarue, J., Dudzinski, K., Hatch, L., Hildebrand, J., Hodge, L., Klinck, H., Kraus, S., ... Van Parijs, S. M. (2017). Long-term passive acoustic recordings track the changing distribution of North Atlantic right whales (*Eubalaena glacialis*) from 2004 to 2014. *Scientific Reports*, 7, 13460. <https://doi.org/10.1038/s41598-017-13359-3>
- Delignette-Muller, M. L., & Dutang, C. (2015). Fitdistrplus: An R package for fitting distributions. *Journal of Statistical Software*, 64(4), 1–34 Retrieved from <http://www.jstatsoft.org/v64/i04/>
- Dunnington, D. (2021). ggspatial: Spatial data framework for ggplot2. R package version 1.1.5. Retrieved from <https://CRAN.R-project.org/package=ggspatial>
- Durette-Morin, D. (2021). *Measuring the distribution of North Atlantic right whales (Eubalaena glacialis) across multiple scales from their vocalizations: Applications for ecology and management* [Master's thesis, Dalhousie University, Halifax, NS]. Retrieved from <http://hdl.handle.net/10222/80343>
- Durette-Morin, D., Davies, K. T. A., Johnson, H. D., Brown, M. W., Moors-Murphy, H., Martin, B., & Taggart, C. T. (2019). Passive acoustic monitoring predicts daily variation in North Atlantic right whale presence and relative abundance in Roseway Basin, Canada. *Marine Mammal Science*, 35(4), 1280–1303. <https://doi.org/10.1111/mms.12602>
- Fisheries and Ocean Canada (DFO). (2008). *Protecting the right whale in the North-Atlantic Ocean*. Retrieved from <https://www.dfo-mpo.gc.ca/species-especes/publications/sara-lep/recovering-retablissement/2008-08-eng.html>
- Fisheries and Ocean Canada (DFO). (2020). *Fisheries Management Measures to Protect North Atlantic Right Whales in Canadian Waters*. Retrieved from: <https://www.dfo-mpo.gc.ca/fisheries-peches/commercial-commerciale/atl-arc/narw-bnan/2020/right-whale-baleine-noires-0508-eng.html>
- Fisheries and Oceans Canada (DFO). (2021a). *Action Plan for the North Atlantic Right Whale (Eubalaena glacialis) in Canada. Species at Risk Act Action Plan Series* (p. 46). Fisheries and Oceans Canada Retrieved from <https://www.canada.ca/en/environment-climate-change/services/species-risk-public-registry/action-plans/north-atlantic-right-whale-2021.html#shr-pg0>
- Fisheries and Ocean Canada (DFO). (2021b). *Fishery Notices Related to North Atlantic Right Whales*. Retrieved from: <https://www.dfo-mpo.gc.ca/fisheries-peches/commercial-commerciale/atl-arc/narw-bnan/index-eng.html#impacts>
- Franklin, K. J., Cole, T. V. N., Cholewiak, D. M., Duley, P. A., Crowe, L. M., Hamilton, P. K., Knowlton, A. R., Taggart, C. T., & Johnson, H. D. (2022). Using sonobuoys and visual surveys to characterize North Atlantic right whales (*Eubalaena glacialis*) calling behavior in the Gulf of St. Lawrence. *Endangered Species Research*, 49, 159–174. <https://doi.org/10.3354/esr01208>
- Ganley, L., Brault, S., & Mayo, C. (2019). What we see is not what there is: Estimating North Atlantic right whale *Eubalaena glacialis* local abundance. *Endangered Species Research*, 38, 101–113. <https://doi.org/10.3354/esr00938>
- Grolemund, G., & Wickham, H. (2011). Dates and times made easy with lubridate. *Journal of Statistical Software*, 40(3), 1–25 Retrieved from <http://www.jstatsoft.org/v40/i03/>
- Hijmans, R. J. (2020). raster: Geographic data analysis and modeling. R package version, 3.1-5. Retrieved from <https://CRAN.R-project.org/package=raster>
- Johnson, H. D., Baumgartner, M., & Taggart, C. T. (2020). Estimating North Atlantic right whale (*Eubalaena glacialis*) location uncertainty following visual or acoustic detection to inform dynamic management. *Conservation Science & Practice*, 2(10), e267. <https://doi.org/10.1111/csp.2.267>
- Johnson, H. D., Morrison, D., & Taggart, C. T. (2021). WhaleMap: A tool to collate and display whale survey results in near real-time. *Journal of Open Source Software*, 6(62), 3094. <https://doi.org/10.21105/joss.03094>
- Johnson, H. D., Taggart, C. T., Newhall, A. E., Lin, Y. T., & Baumgartner, M. F. (2022). Acoustic detection range of right whale upcalls identified in near-real time from a moored buoy and a Slocum glider. *The Journal of the Acoustical Society of America*, 151(4), 2558–2575. <https://doi.org/10.1121/10.0010124>
- Marques, T., Munger, L., Thomas, L., Wiggins, S., & Hildebrand, J. (2011). Estimating North Pacific right whale *Eubalaena japonica* density using passive acoustic cue counting. *Endangered Species Research*, 13, 163–172. <https://doi.org/10.3354/esr00325>
- Marques, T. A., Thomas, L., Martin, S. W., Mellinger, D. K., Ward, J. A., Moretti, D. J., Harris, D., & Tyack, P. L. (2013). Estimating animal population density using passive acoustics. *Biological Reviews*, 88(2), 287–309. <https://doi.org/10.1111/brv.12001>
- Matthews, J., Brown, S., Gillespie, D., Johnson, M., McInaghan, R., Moscrop, A., Nowacek, D., Leaper, R., Lewis, T., & Tyack, P. (2001). Vocalisation rates of the North Atlantic right whale. *Journal of Cetacean Research and Management*, 3(3), 271–282 Retrieved from <https://www.researchgate.net/publication/268273193>
- Mazerolle, M. J. (2020). AICcmodavg: Model selection and multimodel inference based on (Q)AIC(c). R package version 2.3-1. Retrieved from <https://cran.r-project.org/package=AICcmodavg>
- McLane, A. J., Semeniuk, C., McDermond, G. J., & Marceau, D. J. (2011). The role of agent-based models in wildlife ecology and management. *Ecological Modelling*, 222, 1544–1556. <https://doi.org/10.1016/j.ecolmodel.2011.01.020>
- Monsarrat, S., Pennino, M. G., Smith, T. D., Reeves, R. R., Meynard, C. N., Kaplan, D. M., & Rodrigues, A. S. L. (2016). A spatially explicit estimate of the prewhaling abundance of the endangered North Atlantic right whale. *Conservation Biology*, 30(4), 783–791. <https://doi.org/10.1111/cobi.12664>
- Moore, M. J., Rowles, T. K., Fauquier, D. A., Baker, J. D., Biedron, I., Durban, J. W., Hamilton, P. K., Henry, A. G., Knowlton, A. R., McLellan, W. A., Miller, C. A., Pace, R. M., Pettis, H. M., Raverty, S., Rolland, R. M., Schick, R. S., Sharp, S. M., Smith, C. R., Thomas, L., ... Ziccardi, M. H. (2021). Assessing North Atlantic right whale health: Threats, and development of tools critical for conservation of the species. *Diseases of Aquatic Organisms*, 143, 205–226. <https://doi.org/10.3354/dao03578>
- National Oceanographic and Atmospheric Administration (NOAA). (2021). *2017–2021 North Atlantic Right Whale Unusual Mortality Event*. Retrieved from <https://www.fisheries.noaa.gov/national/marine-life-distress/2017-2021-north-atlantic-right-whale-unusual-mortality-event>
- NOAA National Geophysical Data Center. (2009). *ETOPO1 1 Arc-Minute Global Relief Model*. NOAA National Centers for Environmental Information. <https://doi.org/10.7289/V5C8276M>
- Parks, S. E., Brown, M. W., Conger, L. A., Hamilton, P. K., Knowlton, A. R., Kraus, S. D., Slay, C. K., & Tyack, P. L. (2007).

- Occurrence, composition, and potential functions of North Atlantic right whale (*Eubalaena glacialis*) surface active groups. *Marine Mammal Science*, 23(4), 868–887. <https://doi.org/10.1111/j.1748-7692.2007.00154.x>
- Parks, S. E., & Tyack, P. L. (2005). Sound production by North Atlantic right whales (*Eubalaena glacialis*) in surface active groups. *Journal of the Acoustical Society of America*, 117, 3297–3306. <https://doi.org/10.1121/1.1882946>
- Pebesma, E. (2018). Simple features for R: Standardized support for spatial vector data. *R Journal*, 10(1), 439–446. <https://doi.org/10.32614/RJ-2018-009>
- Pebesma, E., & Bivand, R. S. (2005). Classes and methods for spatial data in R. *R News*, 5(2), 9–13. Retrieved from <https://cran.r-project.org/doc/Rnews/>
- Pettis, H. M., Pace, R. M., III, & Hamilton, P. K. (2022). North Atlantic right whale consortium 2021 annual report card. *Report to the North Atlantic Right Whale Consortium*, 2–6. Retrieved from <https://www.narwc.org/report-cards.html>
- R Core Team. (2020). *R: A language and environment for statistical computing*. R Foundation for Statistical Computing Retrieved from <https://www.R-project.org/>
- Record, N. R., Runge, J. A., Pendleton, D. E., Balch, W. M., Davies, K. T. A., Pershing, A. J., Johnson, C. L., Stamieszkin, K., Ji, R., Feng, Z., Kraus, S. D., Kenney, R. D., Hudak, C. A., Mayo, C. A., Chen, C., Salisbury, J. E., & Thompson, C. R. S. (2019). Rapid climate-driven circulation changes threaten conservation of endangered North Atlantic right whales. *Oceanography*, 32(2), 1–8. <https://doi.org/10.5670/oceanog.2019.201>
- Schofield, O., Kohut, J., Aragon, D., Creed, L., Graver, J., Haldeman, C., Kerfoot, J., Roarty, H., Jones, C., Webb, D., & Glenn, S. (2007). Slocum gliders: Robust and ready. *Journal of Field Robotics*, 24, 473–485. <https://doi.org/10.1002/rob.20200>
- Sharp, S. M., McLellan, W. A., Rotstein, D. S., Costidis, A. M., Barco, S. G., Durham, K., Pitchford, T. D., Jackson, K. A., Daoust, P. Y., Wimmer, T., Couture, E. L., Bourque, L., Frasier, T., Frasier, B., Fauquier, D., Rowles, T. K., Hamilton, P. K., Pettis, H., & Moore, M. J. (2019). Gross and histopathologic diagnoses from North Atlantic right whale *Eubalaena glacialis* mortalities between 2003 and 2018. *Diseases of Aquatic Organisms*, 135, 1–31. <https://doi.org/10.3354/dao03376>
- South, A. (2017). rnatuarearth: World map data from natural earth. R package version 0.1.0. Retrieved from <https://CRAN.R-project.org/package=rnatuarearth>
- Thomson, J. A., Cooper, A. B., Burkholder, D. A., Heithaus, M. R., & Dill, L. M. (2013). Correcting for heterogeneous availability bias in surveys of long-diving marine turtles. *Biological Conservation*, 165, 154–161. <https://doi.org/10.1016/j.biocon.2013.06.005>
- Transport Canada (TC). (2020). *Protecting North Atlantic Right Whales From Collision with the Vessels in the Gulf of St. Lawrence*. Retrieved from <https://tc.canada.ca/en/marine-transportation/navigation-marine-conditions/protecting-north-atlantic-right-whales-collisions-vessels-gulf-st-lawrence>
- van der Hoop, J. M., Vanderlaan, A. S. M., & Taggart, C. T. (2012). Absolute probability estimates of lethal vessel-strikes to North Atlantic right whales in Roseway Basin, Scotian Shelf. *Ecological Applications*, 22, 2021–2033 Retrieved from <https://www.jstor.org/stable/41723112>
- Wickham, H. (2016). *ggplot2: Elegant graphics for data analysis*. Springer-Verlag Retrieved from <https://ggplot2.tidyverse.org>
- Wickham, H., Averick, M., Bryan, J., Chang, W., McGowan, L., François, R., Grolemund, G., Hayes, A., Henry, L., Hester, J., Kuhn, M., Pedersen, T., Miller, E., Bache, S., Müller, K., Ooms, J., Robinson, D., Seidel, D., Spinu, V., ... Yutani, H. (2019). Welcome to the tidyverse. *Journal of Open Source Software*, 4(43), 1686. <https://doi.org/10.21105/joss.01686>
- Williams, S., Gende, S., Lukacs, P., & Webb, K. (2016). Factors affecting whale detection from large ships in Alaska with implications for whale avoidance. *Endangered Species Research*, 30, 209–223. <https://doi.org/10.3354/esr00736>
- Zeileis, A., & Grothendieck, G. (2005). Zoo: S3 infrastructure for regular and irregular time series. *Journal of Statistical Software*, 14(6), 1–27. <https://doi.org/10.18637/jss.v014.i06>
- Zitterbart, D. P., Smith, H. R., Flau, M., Richter, S., Burkhardt, E., Beland, J., Bennett, L., Cammareri, A., Davis, A., Holst, M., Lanfredi, C., Michel, H., Noad, M., Owen, K., Pacini, A., & Boebel, O. (2020). Scaling the laws of thermal imaging-based whale detection. *Journal of Atmospheric and Oceanic Technology*, 37, 807–824.

How to cite this article: Ceballos, V., Taggart, C., & Johnson, H. (2023). Comparison of visual and acoustic surveys for the detection and dynamic management of North Atlantic right whales (*Eubalaena glacialis*) in Canada. *Conservation Science and Practice*, 5(2), e12866. <https://doi.org/10.1111/csp2.12866>